



Published in final edited form as:

Genes Chromosomes Cancer. 2021 April ; 60(4): 263–271. doi:10.1002/gcc.22926.

Pediatric fibromyxoid soft tissue tumor with *PLAG1* fusion: A novel entity?

Catherine T. Chung^{1,2}, Cristina R. Antonescu³, Brendan C. Dickson^{2,4}, Rose Chami^{1,2}, Paula Marrano¹, Rong Fan⁵, Mary Shago^{2,6}, Meera Hameed³, Paul S. Thorner²

¹Division of Pathology, The Hospital for Sick Children, Toronto, Canada

²Department of Laboratory Medicine and Pathobiology, University of Toronto, Toronto, Canada

³Department of Pathology, Memorial Sloan Kettering Cancer Center, New York, New York

⁴Department of Pathology and Laboratory Medicine, Mount Sinai Hospital, Toronto, Canada

⁵Division of Pediatric Pathology, Riley Hospital for Children at Indiana University Health, Indianapolis, Indiana

⁶Division of Genome Diagnostics, Department of Pediatric Laboratory Medicine, The Hospital for Sick Children, Toronto, Canada

Abstract

The classification of undifferentiated soft tissue tumors continues to evolve with the expanded application of molecular analysis in clinical practice. We report three cases of a unique soft tissue tumor in young children (5 months to 2 years old) displaying a purely fibromyxoid histology, with positive staining for desmin and CD34. In two cases, RNA sequencing detected a *YWHAZ-PLAG1* gene fusion, while in the third case, a previously unreported *EEF1A1-PLAG1* fusion was identified. *PLAG1* fusions have been reported in several pathologic entities including pleomorphic adenoma, myoepithelial tumors of skin and soft tissue, and lipoblastoma, the latter occurring preferentially in young children. In these tumors, expression of a full length *PLAG1* protein comes under the control of the constitutively active promoter of the partner gene in the fusion, and the current cases conform to that model. Overexpression of *PLAG1* was confirmed by diffusely positive immunostaining for *PLAG1* in all three cases. Our findings raise the possibility of a novel fibromyxoid neoplasm in childhood associated with these rare *PLAG1* fusion variants. The only other report of a *PLAG1-YWHAZ* fusion occurred in a pediatric tumor diagnosed as a “fibroblastic lipoblastoma.” This finding raises the possibility of a relationship with our three cases, even though our cases lacked any fat component. Further studies with regard to a shared pathogenesis are required.

Keywords

EEF1A1 ; lipoblastoma; *PLAG1* ; soft tissue; translocation; tumor; *YWHAZ*

1 | INTRODUCTION

Over the past few decades, it has been determined that many pediatric soft tissue neoplasms possess gene fusions that are diagnostic, or become so in the context of the histopathologic findings of the particular tumor.^{1,2} Yet, there remain tumors that lack morphologies and immunohistochemical profiles distinctive enough to allow a definitive and reproducible diagnosis, and instead are labeled descriptively, such as “unclassified spindle cell neoplasm.” This category is decreasing at an accelerated pace due to the application of more modern molecular genetic techniques including next-generation sequencing panels, anchored multiplex polymerase chain reaction systems to detect the partner for a known fusion gene, and comprehensive RNA sequencing. For example, certain pediatric soft tissue tumors have become recognized due to better characterization at the molecular level including *NTRK*-fusion sarcomas, spindle cell/sclerosing rhabdomyosarcoma, and undifferentiated sarcomas characterized by *BCOR* genetic alterations. Many of the gene fusions involve growth factors (eg, PDGFB) or protein kinases (eg, ALK, ROS, NTRK, BRAF), or abnormal function of transcription factors or chromatin remodeling. In this report, we add three soft tissue tumors with a distinctive mixed myxoid and fibroblastic histology, occurring in young children. Based on morphologic grounds, these tumors did not fit into any well-defined category; however, molecular characterization uncovered unusual *PLAG1*-related fusions, involving *YWHAZ* in two cases, and *EEF1A1* in one other case. Translocations involving *PLAG1* have been known for some time to occur in several tumors including pleomorphic adenoma, skin and soft tissue myoepithelioma, and lipoblastoma.^{3–7} To the best of our knowledge, translocations involving *YWHAZ* have only been reported in two cases to date,^{8,9} one of which occurred in a “fibroblastic lipoblastoma” involving *PLAG1*, while translocations involving *EEF1A1* have been described in four cases,^{10–12} none of which involved *PLAG1*. Thus, the involvement of *YWHAZ* and *EEF1A1* in this fibromyxoid type of pediatric tumor is unique.

2 | PATHOLOGY

2.1 | Case 1

This case was a 2-year-old girl with a 3 week history of a painless left posterior neck mass. The mass was fixed, firm and nontender and there were no palpable lymph nodes. Computed tomography (CT) scan confirmed a well-circumscribed mass ($5.2 \times 3.6 \times 3.0$ cm) in close proximity to the left lamina of vertebra C2, with no evidence of calvarial bone erosion or foraminal or intraspinal extension. An incisional biopsy was performed, followed by a marginal resection of the mass, including the biopsy tract and overlying skin. The mass was circumscribed and located within the deep soft tissue. The patient did not receive adjuvant chemotherapy or radiotherapy and has no evidence of recurrence 2 years after the resection. The tumor was well-demarcated but unencapsulated; the cut surface was white and trabeculated, varying from firm to myxoid in nature. Microscopically, the tumor showed a distinct biphasic morphology with a vaguely plexiform appearance (Figure 1). There were discrete nodules of low-cellularity composed of spindle- to ovoid-shaped cells dispersed within a loose myxoid stroma containing scattered collagen strands and a network of branching, thin-walled vessels. Rare bi- and multinucleated cells were present but, overall,

the cells lacked atypia. These myxoid nodules were separated by areas of a moderately cellular, spindle cell proliferation arranged in intersecting fascicles. There was no significant nuclear pleomorphism. Occasional mitoses were identified (up to 4 per 10 high-power fields), mainly within the more cellular component. Ki-67 labeling index was less than 5%. No necrosis was present and there were scattered inflammatory cells including histiocytes and occasional mast cells. Both components were diffusely immunoreactive for CD34 and desmin. In addition, the spindle cells in the myxoid areas expressed S-100 protein, GFAP, D2–40, CD10, and CD117. BAF47 expression was retained. There was no nuclear staining for beta-catenin. The following immunostains were also negative: SOX10, smooth muscle actin, calponin, actin, BCOR, MUC4, pancytokeratin (AE1/AE3), cytokeratin 18, epithelial membrane antigen, WT1 (NH2 terminal), CD31, calretinin, p63, PGP9.5, neurofilament, and ALK1. The tumor was felt not to correspond to any known entity and was categorized as a low-grade spindle cell neoplasm, awaiting molecular genetic testing.

2.2 | Case 2

This case was a scalp mass resected from a 1-year-old girl. The tumor was a well-circumscribed nodule composed of uniform ovoid and short spindle cells within a predominantly fibrotic stroma, arranged in short fascicles, but also with solid areas, sometimes storiform, or as single files separated by collagen columns (Figure 2). Focal myxoid areas were also noted. The cells had a moderate amount of amphophilic cytoplasm and plump ovoid nuclei with vesicular chromatin and small nucleoli. There was no evidence of atypia or necrosis to suggest malignancy, and mitotic activity was low (1/10 HPFs). Ki-67 proliferation index was 5%. The tumor was diffusely positive for desmin and focally positive for CD34. The following immunostains were negative: smooth muscle actin, myogenin, MyoD1, S-100 protein, beta-catenin, EMA, STAT6, bc12, CD99, ALK-D5, ROS1, and pan-NTRK. The tumor was considered to be a benign myofibroblastic neoplasm, possibly a myofibroma, and molecular genetic testing was performed.

2.3 | Case 3

This case was from a 3-month-old male who presented with a mass on the dorsum of the left foot, increasing in size over the last few days. An incisional biopsy was performed, following by a resection of the mass 1 month later. The excised tumor was a lobulated rubbery mass measuring 4.7 × 3.9 × 2.6 cm. Microscopically, the tumor showed a distinct biphasic morphology with pale myxoid nodules separated by pink fibroblastic areas (Figure 3). The fibroblastic areas were of low cellularity and composed of spindle-shaped cells, with small ovoid nuclei, arranged in short intersecting fascicles. The myxoid areas contained similar appearing spindle-shaped cells embedded within a myxoid amphophilic stroma. There was no atypia or necrosis. Scattered branching thin-walled, occasionally ectatic, vessels were present. The tumor was diffusely positive for desmin, and focally positive for S-100 protein and CD34. The tumor was negative for smooth muscle actin, myogenin, MyoD1, SOX-10, EMA, STAT6, GLUT1, MUC4, and pan-NTRK. Ki-67 showed a proliferative rate of less than 2%. A benign myofibroblastic tumor was the working diagnosis, until molecular testing was completed.

3 | MATERIALS AND METHODS

3.1 | RNA-sequencing (RNA-seq)

RNA-seq was performed for case 1 using the TruSight RNA Fusion Panel as previously described.^{13,14} Briefly, total RNA was extracted from formalin-fixed paraffin-embedded (FFPE) tissue scrolls (3–4 per case) using the ExpressArt FFPE Clear RNA Ready kit (Amsbio, Cambridge, MA). RNA quality was assessed using the RNA 6000 Nano Bioanalyzer Kit (Agilent, Mississauga, ON) and quantitated using the Qubit RNA HS Assay Kit (ThermoFisher Scientific, Mississauga, ON). An input of 20 to 100 ng total RNA and the TruSight RNA Fusion Panel were used to prepare the RNA-seq libraries (Illumina, San Diego, CA), following manufacturer's instructions and as previously described. Sequencing of each sample was performed with 76 basepair paired-end reads on an Illumina MiSeq at eight samples per flow cell (~3 million reads per sample). The results were then analyzed using the STAR and BOWTIE2 aligners, and Manta and JAFFA fusion callers, respectively.

3.2 | Archer FusionPlex assay

Archer FusionPlex-targeted RNA sequencing analysis was performed for cases 2 and 3, as previously described.¹⁵ RNA was extracted from FFPE tumor material followed by cDNA synthesis. cDNA was then subjected to dA tailing, and ligation with Illumina molecular barcode adapters. Ligated fragments were subjected to two rounds of PCR amplification using two sets of gene-specific primers and a primer complementary to the Illumina adapter. Following PCR, the final targeted amplicons were sequenced on an Illumina MiSeq instrument (2 × 150 bp). The Archer analysis software V5.0 was used for data analysis.

3.3 | Cytogenetics and spectral karyotyping

Direct preparations and short-term collagenase-treated cultures were prepared and G-banded according to standard cytogenetic techniques. Spectral karyotyping (SKY) analysis was carried out on the same metaphase preparations used for G-banding. The assay was performed with the SKY probe according to the manufacturer's instructions (Applied Spectral Imaging, Carlsbad, CA) as previously described.¹⁶

3.4 | Fluorescent in situ hybridization

Fluorescent in situ hybridization (FISH) was performed as previously described.¹³ Bacterial artificial chromosome DNA was acquired from the Applied Center for Genomics, Toronto, Canada (<http://www.tcg.ca/>) and selected according to the UCSC Genome Bioinformatics Browser (<http://genome.ucsc.edu/>, GRCh37/hg19 Build). For this case, the following probes were used: RP11–954B4 labeled with spectrum green for the *YWHAZ* gene, and RP11–22I14 labeled with spectrum orange for the *PLAG1* gene. RP11–954B4 is located 21 835 base pairs 5' of the start of exon 1 of *YWHAZ* and RP11–22I14 is located 25 457 base pairs 3' of the end of exon 5 of *PLAG1* (Figure 4). Both *YWHAZ* and *PLAG1* are located on chromosome 8, and on a normal chromosome, the two probes would be separated by 44 854 237 base pairs. The labeled probes were hybridized to normal human lymphocyte metaphases to confirm their chromosomal location. FISH was performed on both the slides used for SKY and FFPE tumor samples.

4 | MOLECULAR GENETIC ANALYSIS

4.1 | Case 1

A diagnosis of low-grade fibromyxoid sarcoma was considered, but interphase FISH analysis with a dual color break-apart probe for the *FUS* gene was negative, as well as reverse transcriptase polymerase chain reaction (RT-PCR) for the t(7;16)(q33;p11) fusion transcript. Using RNA-seq, a fusion was detected between the *YWHAZ* gene (RefSeq NM_145690) at 8q22.3 and the *PLAG1* gene (RefSeq NM_002655) at 8q12.1 (Figure 4). The entire exon 1 of *YWHAZ* was fused to the start of exon 3 of *PLAG1*, implying an interstitial deletion of 44.7 Mb in the long arm of chromosome 8. Exon 1 of *YWHAZ* codes for the 50 untranslated region;¹⁷ coding of the *YWHAZ* protein begins in exon 2 (at nucleotide 105 of mRNA). Coding of the *PLAG1* protein begins in exon 4 (at nucleotide 475 of mRNA);^{6,18} thus, the entire *PLAG1* protein should be expressed in this gene fusion and, indeed, immunostaining for *PLAG1* was diffusely positive in both the myxoid and cellular regions of the tumor (Figure 1).

Karyotype of the tumor by G-banding and SKY showed a gain of 1 to 3 additional copies of chromosome 8 (Figure 5). Most metaphases (85%) had five copies of chromosome 8. No other abnormalities were noted on G-banding. Based on the knowledge of the gene fusion detected by RNA-Seq, the FISH probes for *YWHAZ* and *PLAG1* would be spaced apart by 90 424 bp, rather than the normal spacing of 44 854 237 bp (>99% reduction) and easily distinguished from normal. Using these two probes on metaphase spreads, there was one normal chromosome 8 per metaphase and fusion or close approximation of the two signals in the remaining copies of chromosome 8 (2–4 copies per metaphase). FISH was next performed on interphase nuclei in tissue sections of the resected specimen. Myxoid and cellular regions of the tumor were scored separately, but both regions showed identical results. Chromosome 8 copy number ranged from 2–5/nucleus with four or five copies noted in at least 60% of nuclei. All nuclei showed 0 to 1 normal chromosome 8 and a fused signal in the other copies of chromosome 8 (Figure 6). In addition, a separate break-apart FISH probe for *PLAG1* confirmed the presence of a rearrangement (data not shown).

4.2 | Case 2

By Archer FusionPlex targeted RNA sequencing, a similar fusion to case 1 was detected in case 2 between the *YWHAZ* gene and the *PLAG1* gene. In case 2, however, exon 1 of *YWHAZ* was fused to the start of exon 2 of *PLAG1*, instead of exon 3 as in case 1 (Figure 4). Since coding of the *PLAG1* protein begins in exon 4, the entire *PLAG1* protein should be expressed in this gene fusion. As predicted, immunostaining for *PLAG1* was diffusely positive in the tumor (Figure 2). FISH performed on interphase nuclei showed a fusion signal between *YWHAZ* and *PLAG1* similar to case 1, with chromosome 8 copy number ranging from 2–6/nucleus and one to three copies of the fusion signal per nucleus (results not shown).

4.3 | Case 3

By Archer FusionPlex targeted RNA sequencing, a fusion was detected between the *EEF1A1* gene (RefSeq NM_001402) at 6q13 and the *PLAG1* gene at 8q12.1. The entire

exon 1 of *EEF1A1* was fused to the start of exon 2 of *PLAG1*. Exon 1 of *EEF1A1* codes for the 5' untranslated region; coding of the *EEF1A1* protein begins in exon 2.^{19,20} Thus, as with cases 1 and 2, the entire *PLAG1* protein should be expressed in the gene fusion of case 3, with no protein contribution from the 5' partner. As expected, immunostaining for *PLAG1* was diffusely positive in the tumor (Figure 3).

5 | DISCUSSION

Gene fusions involving *PLAG1* have long been recognized in human neoplasia,^{3–7} whereas fusions involving *YWHAZ* and *EEF1A1* are almost unknown. In *PLAG1*-fusion tumors, expression of a full-length *PLAG1* protein comes under the control of the constitutively active promoter of the partner gene in the fusion. The oncogenic effects of *PLAG1* are believed to be related to upregulation of a wide array of direct target genes, including growth factors, growth factor binding proteins, growth factor receptors, and cell cycle-related proteins. There are two reports documenting a gene fusion involving *YWHAZ*. One bears no resemblance to our two cases; the partner gene was *BRAF* instead of *PLAG1*, the fusion was at exon 5 of *YWHAZ* instead of exon 1, and the tumor was a cholangiocarcinoma in an adult.⁹ The other is a fusion to *PLAG1* similar to our two cases, but occurring in a “fibroblastic lipoblastoma.”⁸ The *YWHAZ* gene is located at 8q22.3 and encodes tyrosine 3-monooxygenase/tryptophan 5-monooxygenase activation protein zeta (14–3-3ζ), which belongs to a family of ubiquitously expressed proteins that bind to phosphoserine- or phosphothreonine-containing target proteins.¹⁷ Through these interactions, *YWHAZ* modulates cell cycle control, protein trafficking, apoptosis, metabolism, and signal transduction.^{17,21–23} The *YWHAZ* gene has six exons; exon 1 encodes the majority of the 5'UTR and the start codon is in exon 2. Thus, in the fusion transcript in our cases, the *YWHAZ* gene contributes its promoter but no portion of the *YWHAZ* protein.

Gene fusions involving *EEF1A1* have only been rarely reported. In all cases, *EEF1A1* was the 5' partner, fused to *HSP90AB1* in two cases of colonic adenocarcinoma,¹⁰ *PDL2* in one case of diffuse large B cell lymphoma in an 18-year-old male,¹² and *RPL32* in a case of CIC-DUX4 sarcoma in an 11-year-old male. In the last case, the fusion was only found in the post-treatment specimen, not the initial biopsy.¹¹ The *EEF1A1* gene encodes Eukaryotic Elongation Factor 1 Alpha 1, which is a ubiquitous protein involved in peptide elongation during mRNA translation. Other functions reported for *EEF1A1* include signal transduction, control of cell proliferation and cell death, and cytoskeleton modulation. It is a negative regulator of p53 and p73, giving it anti-apoptotic properties.²⁴ The gene is located at 6q13 and is composed of eight exons. Exon 1 encodes ~50% of the 50 untranslated region, thus, the fusion in our third case would include the promoter of *EEF1A1* but none of the *EEF1A1* protein. The *EEF1A1* promoter is known to have strong activity in many cell types, resulting from specific sequences within the promoter.^{19,20} Thus, the *EEF1A1* promoter is expected to be driving transcription of the *PLAG1* gene in our case 3, which was confirmed by the diffuse expression of *PLAG1* in the tumor. Our case differs from other published cases that provided details of an *EEF1A1* fusion.^{10,11} In these cases, the fusions were not in-frame resulting in a premature stop codon and no evidence was provided that the *EEF1A1* gene fusions were indeed functional.

PLAG1 (Pleomorphic Adenoma Gene 1) is located on chromosome 8q12 and encodes a zinc finger proto-oncogene. Most of the documented involvement of *PLAG1* in neoplasia occurs through translocations, with *PLAG1* in the 3' position of the gene fusion and a variety of partners in the 5' position. *PLAG1* fusions have been reported in pleomorphic adenoma,^{4,5,18,25–29} carcinoma ex-pleomorphic adenoma,^{4,25,30,31} myoepithelial tumors of skin and soft tissue,^{3,30,32} chondroid syringoma of skin,³³ lipoblastoma,^{4,8,34–40} uterine myxoid mesenchymal tumors,⁴ and T-ALL.⁴¹ Many of the gene partners in *PLAG1* fusions are on chromosome 8, as is *PLAG1*, including: *TCEA1*, *HAS2*, *NDRG1*, *TRPS1 RAB2A*^{27,33,36,37,40} (and *YWHAZ* as in two of our cases), suggesting recombinations within chromosome 8 are not uncommon events in terms of *PLAG1* translocations. Despite the large number of partners involved in *PLAG1* fusions, there is a remarkably consistent theme to these genetic changes; the gene fusion involves either exon 2 or 3 of the *PLAG1* gene (as in our cases). *PLAG1* is composed of 5 exons, with coding starting in exon 4, resulting in a protein of 500 amino acids.^{6,18} Thus, the above translocations involving *PLAG1* maintain the entire coding sequence of *PLAG1*, but the promoter of *PLAG1* is replaced by the one belonging to the 5' partner gene, a situation referred to as promoter swapping.^{4,28,42} In most cases, the 5' partner gene has been shown to be ubiquitously expressed,^{18,26–29,33,34,38,40} resulting in upregulation of *PLAG1* transcription in the tumor. Our three cases with *YWHAZ* or *EEF1A1* as the 5' partners fit this promoter-swapping model, and the diffuse expression of *PLAG1* in all three cases confirms the overexpression of *PLAG1*. *PLAG1* normally functions as a transcriptional regulator, but is not expressed in adult tissues.^{6,18} Presumably, this is due to negative control elements normally in exon 1 of *PLAG1*, which are lost in the case of a translocation³⁶ leading to overexpression of *PLAG1* in tumors. Expression of *PLAG1* can be detected using immunohistochemistry, for example, in pleomorphic adenoma and lipoblastoma.^{4,5,26,43,44} Overexpression of *PLAG1* appears to be oncogenic; in mouse models this leads to tumor development in salivary gland and kidney.^{45,46} An alternate mechanism for *PLAG1* overexpression is via increased copies of the *PLAG1* gene, which has been reported to occur in pleomorphic adenoma, lipoblastoma, and hepatoblastoma.^{28,35,39,47} Copy gains of *PLAG1* fusions are uncommon but have been reported in pleomorphic adenoma.^{28,30} Our cases 1 and 2 both showed increased copies of *PLAG1* and of the *YWHAZ-PLAG1* fusion. The oncogenic effects of *PLAG1* are believed to be related to upregulation of a wide array of direct target genes, including growth factors, growth factor binding proteins, growth factor receptors, and cell cycle-related proteins and, in particular, insulin-like growth factor 2, vascular endothelial growth factor and mitogen-activated protein kinases.^{7,38,42,45,48}

We believe the three cases in this report to be a unique pediatric soft tissue tumor characterized by unusual *PLAG1* fusions. All cases shared a mixed fibroblastic and myxoid morphology, but no other lines of differentiation. Although none showed a distinctive immunoprofile, all expressed CD34 and desmin, and two expressed S-100 protein as well. Co-expression of S-100 protein and CD34 has been reported in several spindle-cell tumors with a variety of gene fusions.^{49–51} In all three cases, the *PLAG1* gene fusion led to overexpression of the *PLAG1* protein, thus these cases can be readily distinguished from many other soft tissue tumors by immunostaining for this protein. We suspect previously such cases would have been diagnosed simply as an “unclassified spindle cell neoplasm”

or similar terminology. A recent report has documented several novel fusion partners for *PLAG1* in a series of lipoblastomas occurring in older children and adults,⁸ including *YWHAZ* that we detected in two of our cases. These fusion partners had not been detected in several previous series based on this tumor.^{4,34,36–38,40} Almost all of the novel partners occurred in tumors that were diagnosed as “fibroblastic lipoblastoma,” which is an unusual histologic pattern, yet one that comprised almost 25% of cases in this series. These cases were defined as having “a predominance of fibrous stroma, largely obscuring the adipocytic nature of the tumor.”⁸ As these tumors were predominantly fibroblastic and occurring in older children and adults, it is possible that such tumors were not recognized as (or considered to be) lipoblastomas in previous series of lipoblastomas and were therefore excluded from genetic analysis. None of our three cases showed evidence of adipocytic differentiation, and two of these included resection specimens, not simply biopsies. On this basis, a diagnosis of lipoblastoma could not be rendered, despite the young age at diagnosis and *PLAG1* gene rearrangements. However, it is possible that the cases reported as “fibroblastic lipoblastoma”⁸ bear a pathogenetic relationship to the three cases in our series. Further genomic studies are needed to determine whether those reported tumors and our cases lie within a single morphologic spectrum. The biologic potential of our cases remains undetermined at present; there has been no recurrence of tumor in our case 1, but the follow up period is only 2 years at this point, and no follow up is available on the other two cases that are more recent.

ACKNOWLEDGMENTS

We thank David Swanson for excellent technical assistance with the RNA-seq testing.

CONFLICT OF INTEREST

The authors have no conflicts of interest to declare. This research did not receive any specific grant from funding agencies in the public, commercial, or not-for-profit sectors.

DATA AVAILABILITY STATEMENT

The data that support the findings of this study are available from the corresponding author upon reasonable request.

REFERENCES

1. Miettinen M, Felisiak-Golabek A, Luina Contreras A, et al. New fusion sarcomas: histopathology and clinical significance of selected entities. *Hum Pathol.* 2019;86:57–65. [PubMed: 30633925]
2. Suurmeijer AJH, Kao YC, Antonescu CR. New advances in the molecular classification of pediatric mesenchymal tumors. *Genes Chromosomes Cancer.* 2018;58(2):100–110. [PubMed: 30187985]
3. Antonescu CR, Zhang L, Shao SY, et al. Frequent *PLAG1* gene rearrangements in skin and soft tissue myoepithelioma with ductal differentiation. *Genes Chromosomes Cancer.* 2013;52(7):675–682. [PubMed: 23630011]
4. Arias-Stella JA 3rd, Benayed R, Oliva E, et al. Novel *PLAG1* gene rearrangement distinguishes a subset of uterine myxoid leiomyosarcoma from other uterine myxoid mesenchymal tumors. *Am J Surg Pathol.* 2019;43(3):382–388. [PubMed: 30489320]
5. Matsuyama A, Hisaoka M, Nagao Y, Hashimoto H. Aberrant *PLAG1* expression in pleomorphic adenomas of the salivary gland: a molecular genetic and immunohistochemical study. *Virchows Arch.* 2011;458 (5):583–592. [PubMed: 21394649]

6. Van Dyck F, Declercq J, Braem CV, Van de Ven WJ. PLAG1, the prototype of the PLAG gene family: versatility in tumour development (review). *Int J Oncol.* 2007;30(4):765–774. [PubMed: 17332914]
7. Voz ML, Mathys J, Hensen K, et al. Microarray screening for target genes of the proto-oncogene PLAG1. *Oncogene.* 2004;23(1):179–191. [PubMed: 14712223]
8. Fritchie K, Wang L, Yin Z, et al. Lipoblastomas presenting in older children and adults: analysis of 22 cases with identification of novel PLAG1 fusion partners. *Mod Pathol.* 2020. 10.1038/s41379-020-00696-4. [Epub ahead of print].
9. Lim HC, Montesion M, Botton T, et al. Hybrid capture-based tumor sequencing and copy number analysis to confirm origin of metachronous metastases in BRCA1-mutant cholangiocarcinoma harboring a novel YWHAZ-BRAF fusion. *Oncologist.* 2018;23(9):998–1003. [PubMed: 29622700]
10. Pira G, Uva P, Scanu AM, et al. Landscape of transcriptome variations uncovering known and novel driver events in colorectal carcinoma. *Sci Rep.* 2020;10:1–12. [PubMed: 31913322]
11. Ricker CA, Berlow NE, Crawford KA, et al. Undifferentiated small round cell sarcoma in a young male: a case report. *Cold Spring Harb Mol Case Stud.* 2020;6(1):1–22.
12. Van Roosbroeck K, Ferreiro JF, Tousseyn T, et al. Genomic alterations of the JAK2 and PDL loci occur in a broad spectrum of lymphoid malignancies. *Genes Chromosomes Cancer.* 2016;55(5):428–441. [PubMed: 26850007]
13. Chung CT, Marrano P, Swanson D, Dickson BC, Thorner PS. Fusion of ALK to the melanophilin gene MLPH in pediatric spitz nevi. *Hum Pathol.* 2019;87:57–64. [PubMed: 30857967]
14. Dickson BC, Sung YS, Rosenblum MK, et al. NUTM1 gene fusions characterize a subset of undifferentiated soft tissue and visceral tumors. *Am J Surg Pathol.* 2018;42(5):636–645. [PubMed: 29356724]
15. Agaram NP, Zhang L, Cotzia P, Antonescu CR. Expanding the spectrum of genetic alterations in pseudomyogenic hemangioendothelioma with recurrent novel ACTB-FOSB gene fusions. *Am J Surg Pathol.* 2018;42(12):1653–1661. [PubMed: 30256258]
16. Zielenska M, Bayani J, Pandita A, et al. Comparative genomic hybridization analysis identifies gains of 1p35_p36 and chromosome 19 in osteosarcoma. *Cancer Genet Cytogenet.* 2001;130(1):14–21. [PubMed: 11672768]
17. Kasinski A, Dong X, Khuri FR, Boss J, Fu H. Transcriptional regulation of YWHAZ, the gene encoding 14–3-3zeta. *PLoS ONE.* 2014;9(4): e93480. [PubMed: 24690670]
18. Kas K, Voz ML, Roijer E, et al. Promoter swapping between the genes for a novel zinc finger protein and beta-catenin in pleiomorphic adenomas with t(3;8)(p21;q12) translocations. *Nat Genet.* 1997;15(2):170–174. [PubMed: 9020842]
19. Shibui-Nihei A, Ohmori Y, Yoshida K, et al. The 50 terminal oligopyrimidine tract of human elongation factor 1A-1 gene functions as a transcriptional initiator and produces a variable number of us at the transcriptional level. *Gene.* 2003;311:137–145. [PubMed: 12853148]
20. Uetsuki T, Naito A, Nagata S, Kaziro Y. Isolation and characterization of the human chromosomal gene for polypeptide chain elongation factor-1 alpha. *J Biol Chem.* 1989;264(10):5791–5798. [PubMed: 2564392]
21. Lin M, Morrison CD, Jones S, Mohamed N, Bacher J, Plass C. Copy number gain and oncogenic activity of YWHAZ/14–3-3zeta in head and neck squamous cell carcinoma. *Int J Cancer.* 2009;125(3): 603–611. [PubMed: 19405126]
22. Shi J, Ye J, Fei H, et al. YWHAZ promotes ovarian cancer metastasis by modulating glycolysis. *Oncol Rep.* 2019;41(2):1101–1112. [PubMed: 30535456]
23. Watanabe N, Komatsu S, Ichikawa D, et al. Overexpression of YWHAZ as an independent prognostic factor in adenocarcinoma of the esophago-gastric junction. *Am J Cancer Res.* 2016;6(11):2729–2736. [PubMed: 27904785]
24. Blanch A, Robinson F, Watson IR, Cheng LS, Irwin MS. Eukaryotic translation elongation factor 1-alpha 1 inhibits p53 and p73 dependent apoptosis and chemotherapy sensitivity. *PLoS ONE.* 2013;8(6): 1–7.
25. Asahina M, Saito T, Hayashi T, Fukumura Y, Mitani K, Yao T. Clinicopathological effect of PLAG1 fusion genes in pleomorphic adenoma and carcinoma ex pleomorphic adenoma

- with special emphasis on histological features. *Histopathology*. 2019;74(3):514–525. [PubMed: 30307055]
26. Asp J, Persson F, Kost-Alimova M, Stenman G. CHCHD7-PLAG1 and TCEA1-PLAG1 gene fusions resulting from cryptic, intrachromosomal 8q rearrangements in pleomorphic salivary gland adenomas. *Genes Chromosomes Cancer*. 2006;45(9):820–828. [PubMed: 16736500]
 27. Astrom AK, Voz ML, Kas K, et al. Conserved mechanism of PLAG1 activation in salivary gland tumors with and without chromosome 8q12 abnormalities: identification of SII as a new fusion partner gene. *Cancer Res*. 1999;59(4):918–923. [PubMed: 10029085]
 28. Persson F, Winnes M, Andren Y, et al. High-resolution array CGH analysis of salivary gland tumors reveals fusion and amplification of the FGFR1 and PLAG1 genes in ring chromosomes. *Oncogene*. 2008; 27(21):3072–3080. [PubMed: 18059337]
 29. Voz ML, Astrom AK, Kas K, Mark J, Stenman G, Van de Ven WJ. The recurrent translocation t(5;8)(p13;q12) in pleomorphic adenomas results in upregulation of PLAG1 gene expression under control of the LIFR promoter. *Oncogene*. 1998;16(11):1409–1416. [PubMed: 9525740]
 30. Dalin MG, Katabi N, Persson M, et al. Multi-dimensional genomic analysis of myoepithelial carcinoma identifies prevalent oncogenic gene fusions. *Nat Commun*. 2017;8(1):1197–1209. [PubMed: 29084941]
 31. Katabi N, Ghossein R, Ho A, et al. Consistent PLAG1 and HMGA2 abnormalities distinguish carcinoma ex-pleomorphic adenoma from its de novo counterparts. *Hum Pathol*. 2015;46(1):26–33. [PubMed: 25439740]
 32. Bahrami A, Dalton JD, Krane JF, Fletcher CD. A subset of cutaneous and soft tissue mixed tumors are genetically linked to their salivary gland counterpart. *Genes Chromosomes Cancer*. 2012;51(2):140–148. [PubMed: 22038920]
 33. Panagopoulos I, Gorunova L, Andersen K, et al. NDRG1-PLAG1 and TRPS1-PLAG1 fusion genes in chondroid syringoma. *Cancer Genomics Proteomics* 2020;17(3):237–248. [PubMed: 32345665]
 34. Deen M, Ebrahim S, Schloff D, Mohamed AN. A novel PLAG1-RAD51L1 gene fusion resulting from a t(8;14)(q12;q24) in a case of lipoblastoma. *Cancer Genet*. 2013;206(6):233–237. [PubMed: 23890983]
 35. Gisselsson D, Hibbard MK, Dal Cin P, et al. PLAG1 alterations in lipoblastoma: involvement in varied mesenchymal cell types and evidence for alternative oncogenic mechanisms. *Am J Pathol*. 2001;159 (3):955–962. [PubMed: 11549588]
 36. Hibbard MK, Kozakewich HP, Dal Cin P, et al. PLAG1 fusion oncogenes in lipoblastoma. *Cancer Res*. 2000;60(17):4869–4872. [PubMed: 10987300]
 37. Morerio C, Rapella A, Rosanda C, et al. PLAG1-HAS2 fusion in lipoblastoma with masked 8q intrachromosomal rearrangement. *Cancer Genet Cytogenet*. 2005;156(2):183–184. [PubMed: 15642402]
 38. Nitta Y, Miyachi M, Tomida A, et al. Identification of a novel BOC-PLAG1 fusion gene in a case of lipoblastoma. *Biochem Biophys Res Commun*. 2019;512(1):49–52. [PubMed: 30857637]
 39. Warren M, Turpin BK, Mark M, Smolarek TA, Li X. Undifferentiated myxoid lipoblastoma with PLAG1-HAS2 fusion in an infant; morphologically mimicking primitive myxoid mesenchymal tumor of infancy (PMMTI)-diagnostic importance of cytogenetic and molecular testing and literature review. *Cancer Genet*. 2016;209(1–2):21–29. [PubMed: 26701195]
 40. Yoshida H, Miyachi M, Ouchi K, et al. Identification of COL3A1 and RAB2A as novel translocation partner genes of PLAG1 in lipoblastoma. *Genes Chromosomes Cancer*. 2014;53(7):606–611. [PubMed: 24700772]
 41. Atak ZK, Gianfelici V, Hulselmans G, et al. Comprehensive analysis of transcriptome variation uncovers known and novel driver events in T-cell acute lymphoblastic leukemia. *PLoS Genet*. 2013;9(12):e1003997. [PubMed: 24367274]
 42. Juma AR, Damdimopoulou PE, Grommen SV, Van de Ven WJ, De Groef B. Emerging role of PLAG1 as a regulator of growth and reproduction. *J Endocrinol*. 2016;228(2):R45–R56. [PubMed: 26577933]
 43. Katabi N, Xu B, Jungbluth AA, et al. PLAG1 immunohistochemistry is a sensitive marker for pleomorphic adenoma: a comparative study with PLAG1 genetic abnormalities. *Histopathology*. 2018;72(2): 285–293. [PubMed: 28796899]

44. Matsuyama A, Hisaoka M, Hashimoto H. PLAG1 expression in mesenchymal tumors: an immunohistochemical study with special emphasis on the pathogenetical distinction between soft tissue myoepithelioma and pleomorphic adenoma of the salivary gland. *Pathol Int.* 2012;62(1):1–7. [PubMed: 22192798]
45. Chen KS, Stroup EK, Budhipramono A, et al. Mutations in microRNA processing genes in Wilms tumors derepress the IGF2 regulator PLAG1. *Genes Dev.* 2018;32(15–16):996–1007. [PubMed: 30026293]
46. Declercq J, Van Dyck F, Braem CV, et al. Salivary gland tumors in transgenic mice with targeted PLAG1 proto-oncogene overexpression. *Cancer Res.* 2005;65(11):4544–4553. [PubMed: 15930271]
47. Zatkova A, Rouillard JM, Hartmann W, et al. Amplification and overexpression of the IGF2 regulator PLAG1 in hepatoblastoma. *Genes Chromosomes Cancer.* 2004;39(2):126–137. [PubMed: 14695992]
48. Patz M, Pallasch CP, Wendtner CM. Critical role of microRNAs in chronic lymphocytic leukemia: overexpression of the oncogene PLAG1 by deregulated miRNAs. *Leuk Lymphoma.* 2010;51(8):1379–1381. [PubMed: 20687796]
49. Kao YC, Suurmeijer AJH, Argani P, et al. Soft tissue tumors characterized by a wide spectrum of kinase fusions share a lipofibromatosis-like neural tumor pattern. *Genes Chromosomes Cancer.* 2020;59(10):575–583. [PubMed: 32506523]
50. Lopez-Nunez O, Surrey LF, Alaggio R, Fritchie KJ, John I. Novel PPP1CB-ALK fusion in spindle cell tumor defined by S100 and CD34 coexpression and distinctive stromal and perivascular hyalinization. *Genes Chromosomes Cancer.* 2020;59(8):495–499. [PubMed: 32222087]
51. Sheng SJ, Li JM, Zou YF, et al. A low-grade malignant soft tissue tumor with S100 and CD34 co-expression showing novel CDC42SE2-BRAF fusion with distinct features. *Genes Chromosomes Cancer.* 2020;59(10):595–600. [PubMed: 32447786]

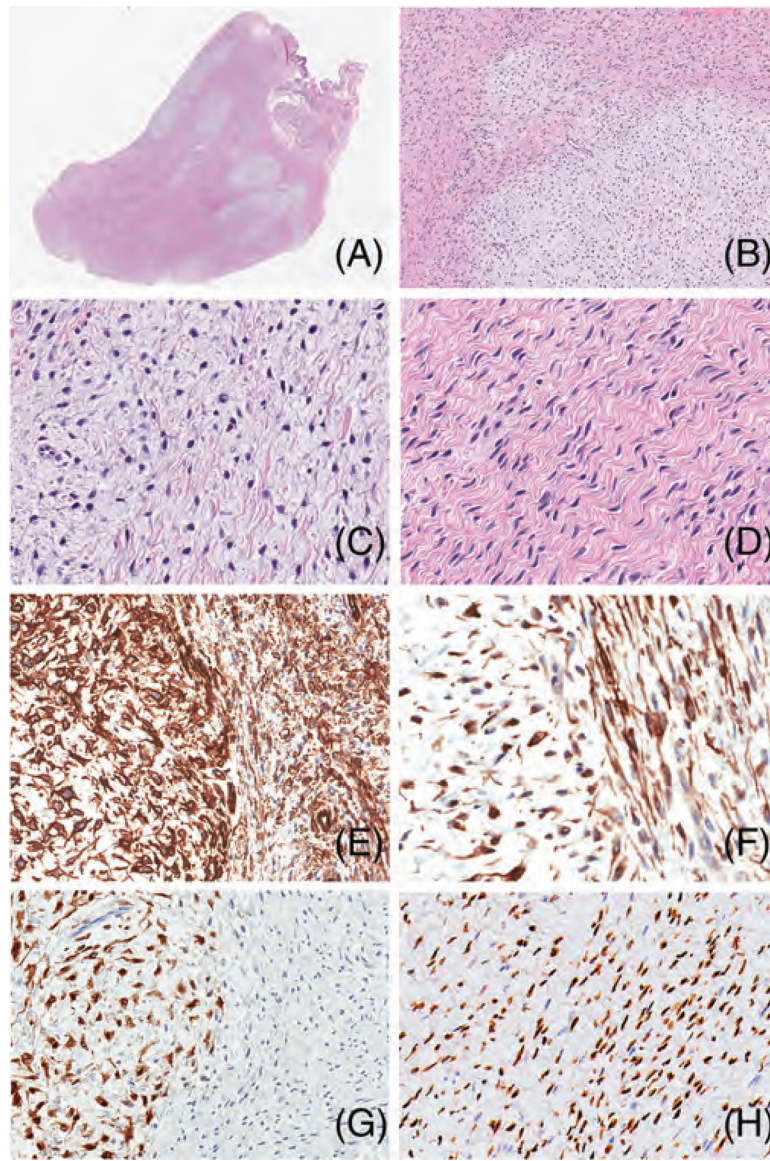


FIGURE 1.

Histologic appearance of the tumor from case 1. A and B, The tumor shows a distinct biphasic morphology with discrete nodules of low cellularity separated by areas of a moderately cellular, spindle cell proliferation. C, The low-cellularity areas are composed of spindle- to ovoid-shaped cells dispersed within a loose myxoid stroma containing scattered collagen strands. D, The more cellular areas are composed of spindle cells arranged in intersecting fascicles. Neither component shows significant atypia or necrosis. E-H, Immunohistochemistry of the two regions with the myxoid area on the left side and the cellular area on the right side, in each panel. There is expression by both components for CD34 (E) and desmin (F) but only the myxoid areas express S-100 protein (G). There is diffuse nuclear expression of PLAG1 (H). (Original magnifications A x1, B x40, C-H x200)

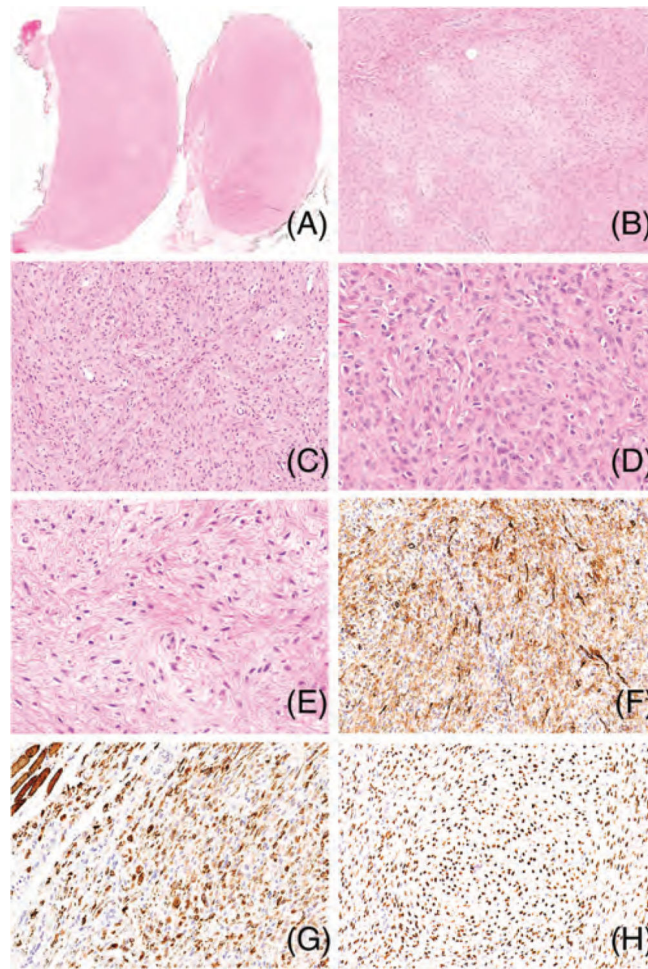


FIGURE 2.

Histologic appearance of the tumor from case 2. A, The tumor is a well-circumscribed nodule and B, shows a predominantly fibroblastic morphology with focal myxoid areas. C, The tumor is composed of uniform ovoid and short spindle cells within a predominantly fibrotic stroma, arranged in short fascicles, but also with solid areas. D, The cells have plump ovoid nuclei with vesicular chromatin and small nucleoli. There is no evidence of atypia or necrosis, and mitotic activity is low. E, The myxoid areas are composed of smaller, ovoid cells within a loose myxoid stroma. F, The tumor is positive for CD34 and G, desmin. H, There is diffuse expression of PLAG1. (Original magnifications A x1, B x40, C-H x200)

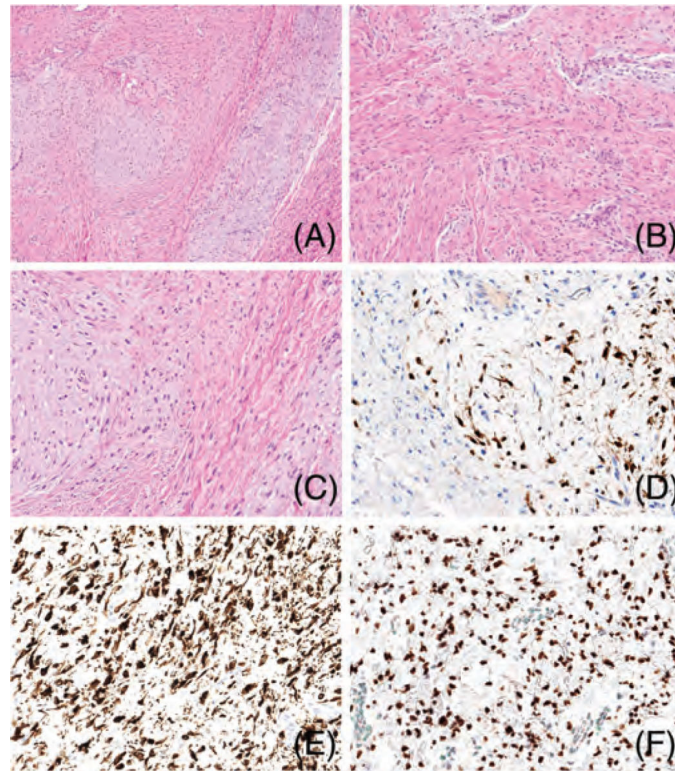


FIGURE 3.

Histologic appearance of the tumor from case 3. A, The tumor shows a biphasic morphology with myxoid nodules separated by fibroblastic areas. B, The fibroblastic areas are paucicellular and composed of small ovoid cells lacking atypia, separated by a moderate amount of collagen. C, The myxoid areas are composed of similar ovoid cells separated by a myxoid amphophilic stroma. D, The tumor is focally positive for S-100 protein and E, diffusely positive for desmin. F, There is diffuse expression of PLAG1. (Original magnifications A x40, B x100, C-H x200)

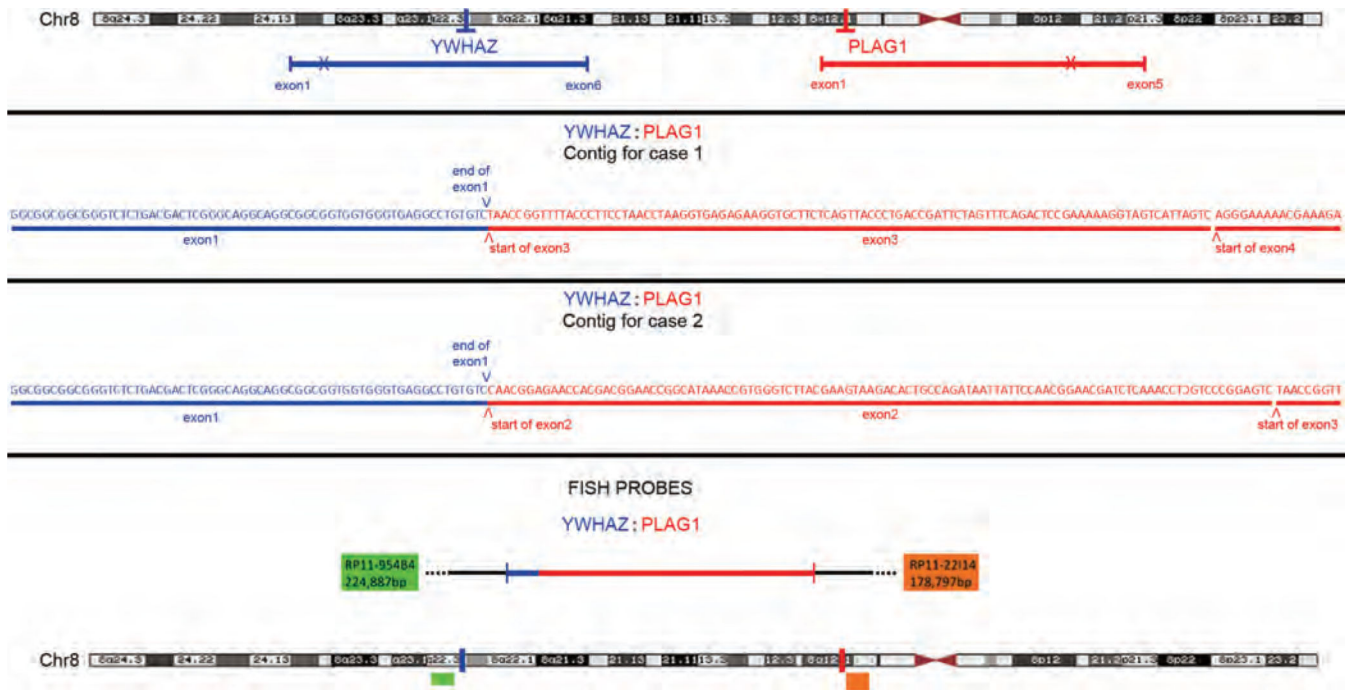


FIGURE 4.

Diagram of fusion transcript of cases 1 and 2 and fluorescent in situ hybridization (FISH) probes. (Top panel) Normal chromosome 8 showing locations of *PLAG1* gene (red) and *YWHAZ* gene (blue). (Second panel) Abnormal transcript detected in case 1 by RNA-Seq, in which exon 1 of *YWHAZ* (blue) (5' end) is fused to exon 3 of *PLAG1* (red) (3' end). (Third panel) Abnormal transcript detected in case 2 by RNA-Seq, in which exon 1 of *YWHAZ* (blue) (5' end) is fused to exon 2 of *PLAG1* (red) (3' end). (Bottom panel) Location of FISH probes RP11–22I14 (labeled with spectrum orange) and RP11–954B4 (labeled with spectrum green) relative to the *PLAG1* and *YWHAZ* genes, respectively

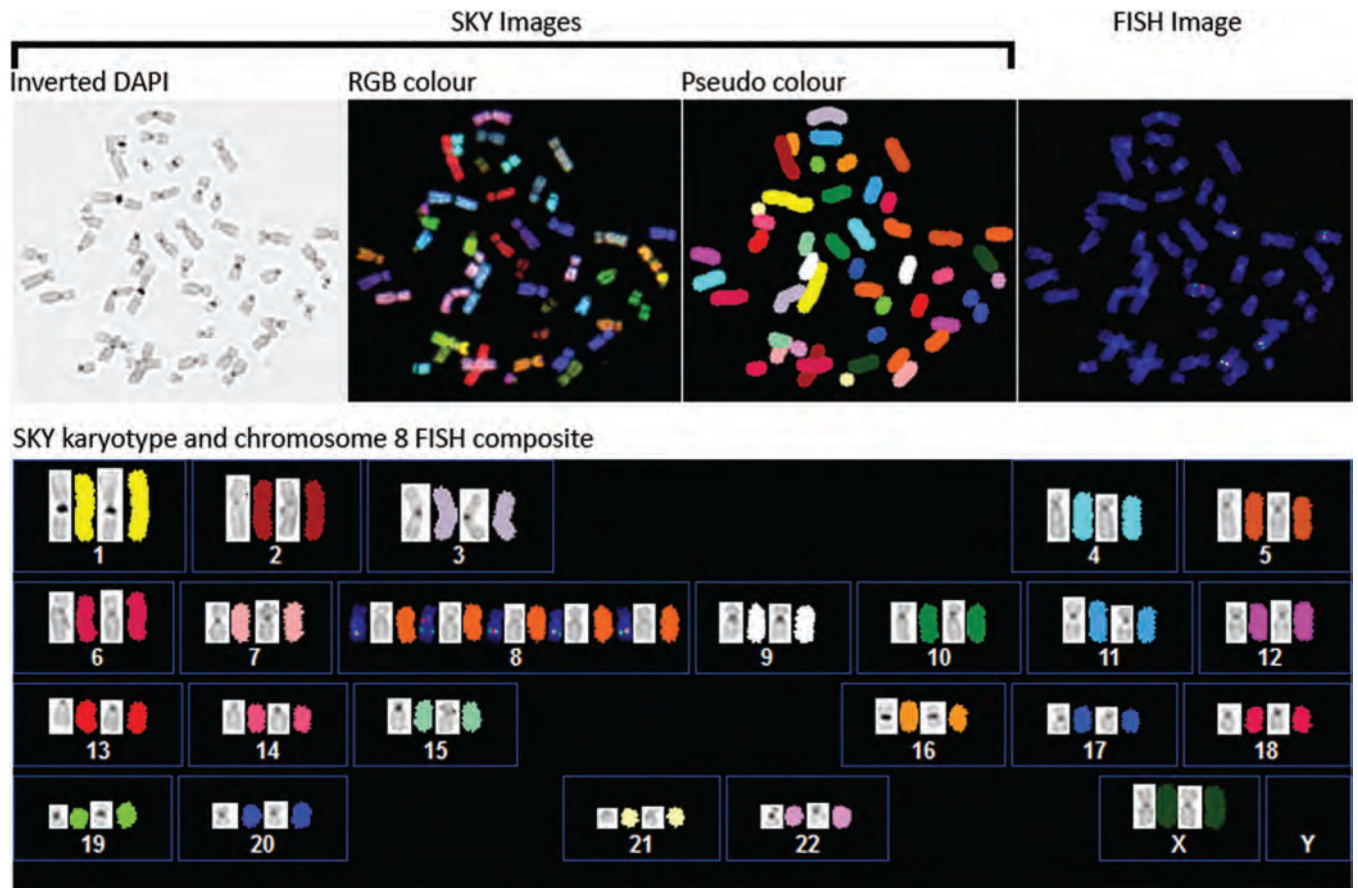


FIGURE 5.

SKY and metaphase FISH results. SKY on the illustrated metaphase spread shows 5 copies of chromosome 8. By FISH on the same metaphase spread, there is close approximation or fusion of the signals of the probes for *PLAG1* (orange) and *YWHAZ* (green) in 4 of the 5 chromosomes 8, in keeping with the fusion transcript detected by RNA-Seq. The remaining chromosome 8 shows a normal FISH pattern. FISH, fluorescent in situ hybridization; SKY, spectral karyotyping

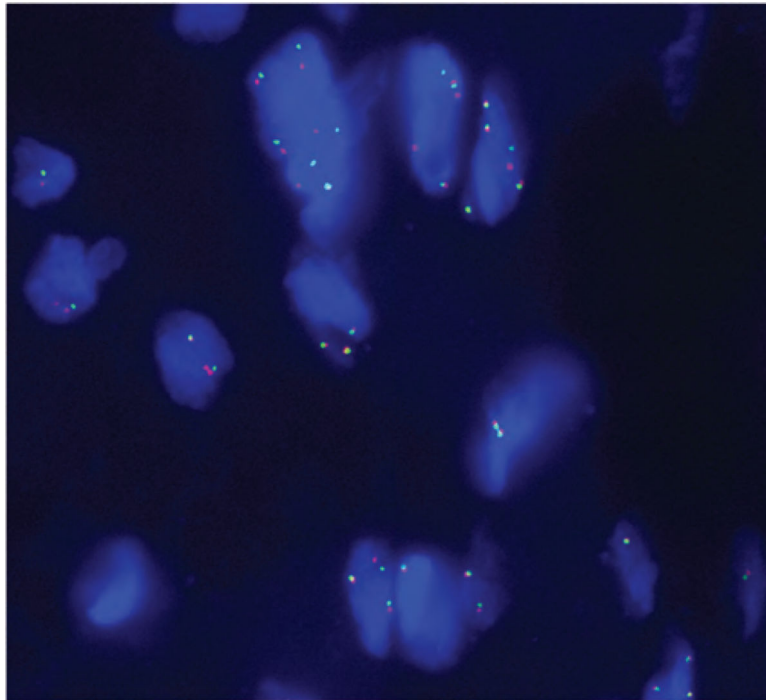


FIGURE 6.

Interphase FISH results. FISH performed in interphase tumor nuclei of case 1 showed identical results for the myxoid and fibroblastic regions of the tumor. There is close approximation or fusion of the signals of the probes for *PLAG1* (orange) and *YWHAZ* (green), in keeping with the fusion transcript detected by RNA-Seq. Multiple copies of the fusion gene are noted in some nuclei. The orange and green probes further apart from each other represent the normal chromosome 8. FISH, fluorescent in situ hybridization